Macromolecules

Article

Functionalizing Polystyrene with *N*-Alicyclic Piperidine-Based Cations *via* Friedel−Crafts Alkylation for Highly Alkali-Stable Anion-Exchange Membranes

Joel S. Olsson, Thanh Huong Pham, and Patric Jannasch*

Read Online

ACCESS | Metrics & More | Article Recommendations | SI Supporting Information

ABSTRACT: Different anion-exchange membranes (AEMs) based on polystyrene (PS)-carrying benzyltrimethyl ammonium cations are currently being developed for use in alkaline fuel cells and water electrolyzers. However, the stability in relation to these state-of-the-art cations needs to be further improved. Here, we introduce highly alkali-stable mono- and spirocyclic piperidine-based cations onto PS by first performing a superacid-mediated Friedel−Crafts alkylation using 2-(piperidine-4-yl)propane-2-ol. This is followed by quaternization of the piperidine rings either using iodomethane to produce *N,N*-dimethyl piperidinium cations or by cyclo-quaternizations using 1,5-dibromopentane and 1,4-dibromobutane, respectively, to obtain *N*-spirocyclic quaternary ammonium cations. Thus, it is possible to functionalize up to 27% of the styrene units with piperidine rings and subsequently achieve complete quaternization. The synthetic approach ensures that all of the sensitive β-hydrogens of the cations are present in ring structures to provide high stability. AEMs based on these polymers show high alkaline stability and less than 5% ionic loss was observed by ^{1}H NMR spectroscopy after 30 days in 2 M aq NaOH at 90 °C. AEMs functionalized with *N,N*-dimethyl piperidinium cations show higher stability than the ones carrying *N*-spirocyclic quaternary ammonium. Careful analysis of the latter revealed that the rings formed in the cyclo-quaternization are more prone to degrade *via* Hofmann elimination than the rings introduced in the Friedel−Crafts reaction. AEMs with an ion-exchange capacity of 1.5 mequiv g^{-1} reach a hydroxide conductivity of 106 mS cm^{-1} at 80 °C under fully hydrated conditions. The AEMs are further tuned and improved by blending with polybenzimidazole (PBI). For example, an AEM containing 2 wt % PBI shows reduced water uptake and much improved robustness during handling and reaches 71 mS cm^{-1} at 80 °C. The study demonstrates that the critical alkaline stability of PS-containing AEMs can be significantly enhanced by replacing the benchmark benzyltrimethyl ammonium cations with *N*-alicyclic piperidine-based cations.

Polystyrene tethered with alicyclic quaternary ammonium cations having:
- No additional heteroatoms
- All β-hydrogens in ring systems
- Fully substituted benzylic positions
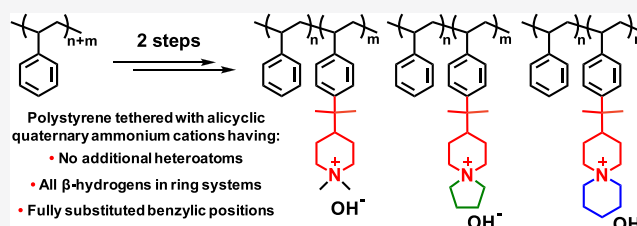
■ INTRODUCTION

Extensive research efforts are currently being directed toward the development of new ionic polymers for use as polymer electrolyte membranes in a variety of different energy storage and conversion devices.[1] The precise molecular structure and properties of these critical components strongly affect the performance and lifetime of the devices.[1] A large number of different cationic polymers have been prepared and studied as anion-exchange membranes (AEMs) primarily for alkaline fuel cells (AEMFCs) but also for water electrolyzers and flow batteries.[1−7] The AEMFC shows some distinct advantages over proton-exchange membrane fuel cells (PEMFCs), which are currently on the brink of mass production. The alkaline operating conditions of the AEMFC result in fewer corrosion issues and faster reaction kinetics, which potentially enable the use of non-platinum group metals, *e.g*, Ni or Fe, for the oxidation reaction.[1] This would result in reduced cost of the fuel cell system and less dependence on strategic metals. However, high-performance fuel cell operation under alkaline conditions at elevated temperature requires AEMs with long-

term thermochemical and mechanical stability as well as high hydroxide conductivity. The hydroxide ion is highly chemically reactive and the key challenge here is to follow a synthetic strategy that prevents the degradation of both the ammonium cations and the polymer backbone.

Cationic loss leading to decreased ion-exchange capacity (IEC) and water uptake of the AEM may occur *via* nucleophilic substitutions at α-carbons, β-hydrogen elimination (Hofmann elimination), or other more complex degradation mechanisms.[8,9] A large number of strategies to mitigate the stability issues of AEMs have been reported recently.[6,8−10] In a seminal work by Marino and Kreuer, certain *N*-alicyclic cations including *N,N*-dimethyl piperidinium and
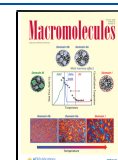
N-spirocyclic quaternary ammonium cations were identified as exceptionally stable.[8] These N-alicyclic cations possessed very high alkaline stability despite having several β-hydrogens available for potential elimination reactions. Their remarkable stability has been ascribed to unfavorable bond angles and lengths in the transition state of E2 reactions, which the ring structure cannot easily accommodate due to geometrical constraints.[8] Recently, it has been reported that N-alicyclic piperidine-based cations degrade predominantly via Hofmann elimination when incorporated into polymers.[11−14] The elimination reaction seems to be accelerated when the relaxation of the ring is restricted by the attachment to stiff aromatic polymer segments.[11,12] For example, poly(arylene piperidinium) functionalized with N-monocyclic and N-spirocyclic ammonium cations showed 8 and 20% ionic losses, respectively, via ring-opening Hofmann elimination reactions during 30 days in 2 M aq NaOH at 90 °C.[11,12]

Polymer chain degradation leads to the gradual loss of viscoelastic properties, which may eventually result in mechanical failure of the AEM. Aryl ether bonds in the polymer backbone are reported to be particularly sensitive to scission reactions, especially in the proximity of electron-withdrawing groups.[15] This finding motivates the use of ether-free polymer backbones, such as poly(arylene alkylene)s[11−14,16−20] and polynorbornenes.[21−24] Polystyrene (PS) is another example of an ether-free polymer that has been extensively investigated for the preparation of AEMs in the form of block and graft copolymers.[25−33] Varcoe et al. have investigated the radiation grafting of poly(vinylbenzyl chloride) onto thin films of ethylene-tetrafluoroethylene (ETFE)[26,27] and low-density polyethylene (LDPE),[28] followed by quaternization with trimethylamine. Recently, fuel cell tests of such AEMs achieved >2 W cm^{-2}, which is one of the highest power densities reported for an AEMFC to date.[28] Moreover, in a number of studies, the PS blocks of PS−poly(ethylene-co-butylene)−PS (SEBS) triblock copolymers have been chloromethylated and then quaternized using trimethylamine.[29−33] In both these approaches, the quaternization results in the formation of benzyltrimethyl ammonium (BTMA) cations (Figure 1a), which are highly activated for degradation by nucleophilic substitution at the benzylic position and may also degrade via anion-induced 1,4-elimination.[8,34] This severely limits the stability and usefulness of AEM-carrying BTMA cations and typically restricts the AEMFC operating conditions. Two

unrelated studies on SEBS functionalized with BTMA reported 19[32] and 28%[33] reductions in IEC, respectively, after 71 and 31 days, respectively, in 1 M aq KOH at 60 °C. Separation of the cation from the benzylic position has proven beneficial both in studies of model compounds[8,9] and in AEMs.[35−42]

Synthetic approaches to improve the ionic stability of AEMs based on PS include the introduction of a spacer unit between the PS backbone and the cation.[35] Bae et al. recently reported on a Friedel−Crafts alkylation reaction to introduce bromoalkyl side chains in the PS blocks of SEBS that were subsequently quaternized with trimethylamine (Figure 1b).[36,37] The AEMs showed good alkaline stability, and both the IEC and OH$^-$ conductivities were retained after testing in a 1 M NaOH solution at 80 °C for 500 h. However, due to the β-hydrogens in the alkyl side chain, the cations may potentially be lost via Hofmann elimination under harsh conditions.[13] Following a different pathway, Li et al. first modified PS via chloromethylation and azidation reactions and then used a Cu(I)-assisted click reaction to attach alkyne-functional N-alicyclic piperidine-based cations to obtain PS samples with the corresponding cations coupled to the backbone via triazole rings (Figure 1c).[38] In this case, the piperidine-based cations were attached in the 4-position, which means that all of the β-hydrogens were located in the six-membered ring structure to impede degradation via Hofmann elimination.[8] ^{1}H NMR analysis of a PS functionalized with N,N-dimethyl piperidinium cations revealed degradation by methyl substitution after storage in 1 M NaOH in CD$_3$OD/D$_2$O at 80 °C, and a corresponding sample with spirocyclic cations showed no degradation under the same conditions after 3000 h.[38] These are excellent results but the synthetic pathway is complex and requires multiple steps.

Inspired by a synthetic approach reported by Bae and coworkers,[36,37,43] here, we report on the straightforward attachment of piperidine-based mono- and spirocyclic quaternary ammonium cations to PS (Figure 1d−f). The first step involves a triflic acid-mediated Friedel−Crafts alkylation of nonmodified PS using commercially available 2-(piperidine-4-yl)propane-2-ol. In the second step, the piperidine rings are quaternized using iodomethane to produce N,N-dimethyl piperidinium cations or cyclo-quaternization reactions are carried out using 1,5-dibromopentane and 1,4-dibromobutane, respectively, to obtain N-spirocyclic quaternary ammonium cations. Notably, none of the tethered piperidine-based cationic moieties contain benzylic protons, or any additional heteroatoms, and are attached in the 4-position. Hence, all of the β-hydrogens are present in six-membered rings to depress degradation by Hofmann elimination. Solvent-cast AEMs were characterized with the primary focus on alkaline and thermal stability as well as hydroxide conductivity. To reduce water uptake and improve mechanical properties, AEMs were also prepared by blending the cationic PS samples with polybenzimidazole (PBI).

RESULTS AND DISCUSSION

PS was functionalized with mono- and spirocyclic piperidinium cations in two steps (Scheme 1). First, 2-(piperidine-4-yl)propan-2-ol (Pip$t$OH) was tethered to commercially available PS (M_n = 170 kg mol^{-1}, PDI = 2.06) in a superacid-mediated Friedel−Crafts alkylation reaction. Here, the aromatic ring in PS reacts with a tertiary carbocation generated after protonation and dissociation of the alcohol moiety in Pip$t$OH. The reaction was carried out in dichloro-
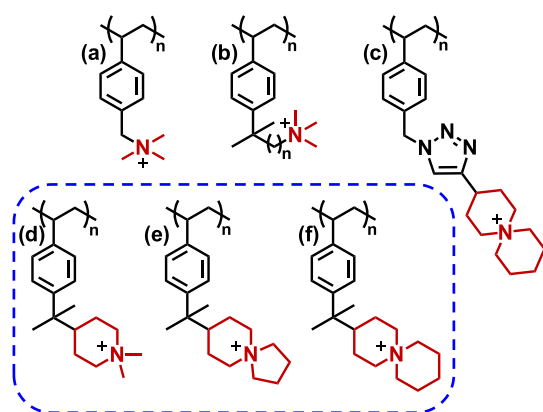
Figure 1. Examples of different quaternary ammonium cations attached to PS. The structures in the blue box were prepared and studied in the present work.

Scheme 1. Synthetic Route to PS-PiQdm, PS-PiQPy, and PS-PiQPi *via* Friedel−Crafts Alkylation, Followed by Different Quaternization Reactions[a]
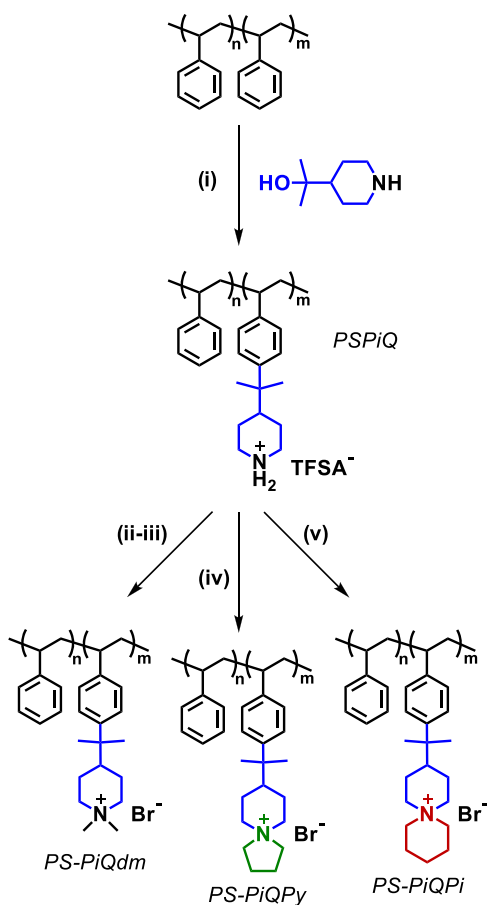
[a]Key: (i) triflic acid, dichloromethane, 0 °C; (ii) iodomethane, K_2CO_3, N-methyl-2-pyrrolidone (NMP), room temperature; (iii) ion-exchange in 1 M NaBr, 50 °C; (iv) 1,4-dibromobutane, N-ethyldiisopropylamine (DIPEA), NMP, 80 °C; and (v) 1,5-dibromopentane, DIPEA, NMP, 80 °C.

Figure 2. ^{1}H NMR spectra of the precursor polymer PS-Pi19 (a) and the quaternized polymers PS-PiQdm-1.4 (b), PS-QPy-1.3 (c), and PS-QPi-1.3 (d). The spectra were recorded with DMSO-d_6 solutions of the samples containing 5−10 vol % 1,1,1-trifluoroacetic acid (TFA).

methane (DCM) at 0 °C. First, a solution of PS and approximately 20 wt % of the Pip*t*OH in DCM was cooled in an ice bath. Upon the addition of trifluoromethanesulfonic acid (TFSA), the solution turned into a turbid red/orange suspension. The rest of the Pip*t*OH was slowly added portionwise over the first hour. As the reaction proceeded, the mixture increased in viscosity, most probably because of the gradual dissolution of the functionalized PS and homogenization of the suspension. After 2 h, the product was precipitated in a 5- to 10-fold volume of diethyl ether, washed once in fresh diethyl ether, and then dried under vacuum at room temperature prior to washing with water and additional drying. Three precursor polymers denoted (PS-Pi*x*) with varying degrees of functionalization (DF, *x*) were prepared (PS-Pi19, PS-Pi22, and PS-Pi27, ^{1}H NMR spectra in Figure S1). The parameter *x* corresponds to the percentage of functionalized styrene units in the polymer and was controlled using a predetermined molar feed ratio of Pip*t*OH per styrene unit.

The ^{1}H NMR spectrum of a representative precursor polymer is shown in Figure 2a. Due to the differences of the equatorial and axial positions, all ring protons produced split

signals (*e.g.*, a and b). With the exception of the protons in the α-position (a) to the charged N-center, all aliphatic protons gave rise to overlapping signals between 0.8 and 2.0 ppm. Since the reaction took place in an acidic medium, the secondary amines in the precursor polymers were protonated ($R_2NH_2^+$), resulting in the appearance of the signals at 8.0−8.6 ppm (f).

The degree of functionalization of the precursor polymers was determined by integration and comparison of the combined aromatic signals and the signals from two of the ring protons at 3.2 ppm (a) in the ^{1}H NMR spectra (Figure 2a). Under the synthetic conditions employed, approximately 50% of the added Pip*t*OH reacted with PS in the functionalization reactions (Table 1) and it was possible to reach degrees of functionalization up to approximately 30%. Attempts to reach higher degrees of functionalization gave products that were insoluble in dimethyl sulfoxide (DMSO), methanol, and N-methyl-2-pyrrolidone (NMP), most probably because of cross-linking.

The glass transition temperatures (T_gs) of the PS-Pi*x* series of precursor polymers were determined by differential scanning calorimetry (DSC) and compared with that of the non-modified high-molecular-weight PS (Figure S2). As expected, the introduction of the bulky piperidine moiety decreased the flexibility of the PS chain and the T_g increased from 105 °C for nonmodified PS to approximately 125 °C for all of the functionalized precursor polymers.

In the second step, cyclo-quaternizations of the PS-Pi19 precursor polymer were carried out using 1,4-dibromobutane

Table 1. Properties of the Functionalized PS Polymers and Their Corresponding AEMs

sample	precursor	$\frac{[PiptOH]}{[S]}$ [a]	DF[b] (%)	IEC$_{NMR}$[c] (mequiv g^{-1})	IEC$_{Titr.}$[d] (mequiv g^{-1})	$T_{d,95}$ (°C)	WU$_{80}$[e] (wt %)		σ_{80}[e] (mS cm^{-1})	
							Br$^-$	OH$^-$	Br$^-$	OH$^-$
PS-PiQdm-1.4	PS-Pi19	0.40	19	1.30	1.26 (1.37)	305	42	85	16	64
PS-PiQdm-1.5	PS-Pi22	0.50	22	1.40	1.37 (1.50)	271	51	120	21	106
PS-PiQdm-1.7	PS-Pi27	0.60	27	1.61	1.56 (1.73)	245	86	268	35	79
PS-PiQPy-1.3	PS-Pi19	0.40	19	1.26	1.23 (1.34)	341	29	70	7	52
PS-PiQPi-1.3	PS-Pi19	0.40	19	1.24	1.22 (1.32)	331	21	53	6	37

[a]Mol PiptOH per mol styrene residues in the reaction feed. [b]Degree of functionalization of the PS-Pix precursors calculated from ^{1}H NMR data of the precursor polymers. [c]In Br$^-$ form, calculated from ^{1}H NMR data. [d]Obtained from Mohr titration of samples in the Br$^-$ form (OH$^-$ form within parentheses). [e]Measured on fully hydrated AEMs at 80 °C in both the Br$^-$ and the OH$^-$ form, respectively.
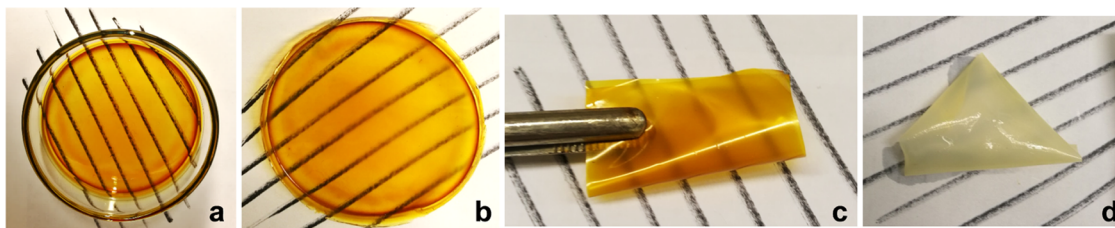
Figure 3. Photographs of PS-PiQdm-1.5 after different treatments in sequence: dry out of the oven in the I$^-$ form (a), after ion-exchange to the Br$^-$ form and washing in water during ~48 h at room temperature (b, c), and after storage in 1 M aq NaOH at room temperature during ~48 h (d).

and 1,5-dibromopentane, respectively, to form polymers carrying N-spirocyclic cations denoted PS-PiQPy-y and PS-PiQPi-y, respectively. In addition, polymers carrying dimethyl piperidinium cations (PS-PiQdm-y) were produced by methylation of the PS-Pix precursors using iodomethane. Here, y denotes the ion-exchange capacity (IEC) in the OH$^-$ form as calculated from the values obtained by Mohr titration. The latter two cations (PiQPi and PiQdm) have been reported to possess excellent alkali stability,[8,11,44] while the former (PiQPy) usually has higher thermal stability.[11,44] ^{1}H NMR spectra of the quaternized polymers are shown in Figure 2b−d. The signals from the protons in the α-position to the charged N-center (1 and 2) were found between 2.7 and 3.7 ppm. All other aliphatic protons gave overlapping signals between 0.8 and 2.0 ppm (Figure 2b−d). After quaternization, complete conversion was verified by the disappearance of the signals from the protonated secondary amines and by comparison of the IEC values calculated from NMR (IEC$_{NMR}$) data with the corresponding data obtained by Mohr titrations (IEC$_{Titr}$, Table 1). Due to the proximity of the overlapping signals between 2.7 and 3.6 ppm in Figure 2b−d and the DMSO-d_6 signal at 2.5 ppm, IEC$_{NMR}$ values were calculated from the degree of functionalization of the precursor polymers to be between 1.24 and 1.61 mequiv g^{-1} (Table 1). The titrated values were between 1.22 and 1.56 mequiv g^{-1}.

AEMs were cast from 5 wt % polymer solutions in DMSO in Petri dishes (Ø = 5 cm) during 48 h at 70 °C. The membranes obtained were fully transparent when dry. The PS AEMs carrying N-spirocyclic cations were brittle and quite difficult to handle when dry, while the dimethyl derivatives were less brittle. All samples became increasingly opaque with the water uptake. This effect can be seen in Figure 3, where photographs of sample PS-PiQdm-1.5 are shown after different treatments. The AEM was fully transparent after casting (a); subsequent ion-exchange to the Br$^-$ form and storage resulted in a more opaque membrane (b). In this form, the material had its best mechanical properties as it was robust and flexible (c). After storage in 1 M aq NaOH, the membrane became fully opaque

and soft (d). This was most probably due to excessive water uptake and the comparatively low T_g of the hydrated AEM.

The thermal decomposition of the AEMs in the Br$^-$ form was studied by thermogravimetric analysis (TGA) under nitrogen. The AEM samples decomposed in one or two steps at decomposition temperatures ($T_{d,95}$) between 245 and 341 °C (Table 1 and Figure S3). The first step most likely originated from the decomposition of the cationic group and the second step corresponded to the decomposition of the PS backbone. AEMs carrying N-spirocyclic cations showed higher thermal stability than the dimethyl derivatives, and the $T_{d,95}$ value of PS-PiQPy-1.3 was 10 °C higher than that of PS-PiQPi-1.3. These general findings agreed well with previous results on, e.g., poly(N,N-diallyldimethylammonium chloride) (poly-DADMAC)-type polyelectrolytes, and poly(arylene alkylenes).[11,44] Because of the high thermal stability of the cation of PS-PiQPy-1.3, this sample decomposed in only one step. In the PS-PiQdm series, an increase in IEC led to a large decrease in thermal stability and hence $T_{d,95}$ of PS-PiQdm-1.3 was 60 °C higher than that of PS-PiQdm-1.7 (Table 1).

Alkaline Stability. The degradation of N-alicyclic piperidine-based cations may occur through several different mechanisms, which all lead to loss of charge and the formation of a tertiary amine, as shown in Scheme 2. To study AEM degradation both quantitatively and qualitatively, the structural changes were monitored by ^{1}H NMR spectroscopy of the polymers after storage in 2 M aq NaOH at 90 and 120 °C during different periods of time. Subsequently, the samples were ion-exchanged to the Br$^-$ form, washed in water, and dried, followed by dissolution in DMSO-d_6 and addition of ~5 to 10 vol % TFA before the ^{1}H NMR analysis. TFA protonated any tertiary amines formed in the degradation, thus enabling quantitative analysis of the total ionic loss. Unfortunately, none of the PS-PiQPy-1.3 samples were soluble after the alkaline treatment and could therefore not be analyzed by NMR spectroscopy. The spectra of PS-PiQdm-1.4 and PS-PiQPi-1.3 before and after alkaline treatment are shown in Figure 4. After 30 days at 90 °C, only minor changes in the spectra were noted

Scheme 2. Degradation Mechanisms of the *N*-Spirocyclic Piperidinium Cation Under Alkaline Conditions[a]
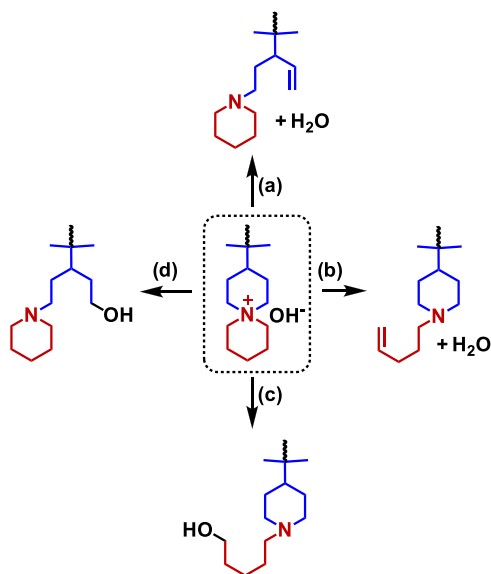
[a]Key: (a, b) ring-opening Hofmann β-elimination and (c, d) ring-opening substitution.

for both AEMs (Figure 4b,e). However, at 120 °C, clear signs of degradation were observed after 10 days of storage for both AEMs (Figure 4c,f). These changes were found in three different specific regions in the ¹H NMR spectra for both samples, denoted I−III in Figure 4. The emerging signals in region II corresponded to vinylic protons (4.5−6 ppm) originating from ring-opening Hofmann β-elimination (Scheme 2a,b). Protonation of tertiary amines formed in degradation reactions by TFA gave rise to the characteristic signal found in region I. The ionic loss detected through the signals in regions I and II was calculated by integration and comparison with the unchanged signals in the aromatic region,

and is shown in Table 2. The changes in region III will be discussed later. After storage at 90 °C, PS-PiQdm-1.4 and PS-

Table 2. Degree of Ionic Loss Calculated from ¹H NMR Data of AEMs Stored in 2 M aq NaOH Under Different Conditions[a]

	30 days at 90 °C		10 days at 120 °C	
sample	region I[b] (%)	region II[c] (%)	region I[b] (%)	region II[c] (%)
PS-PiQ**dm**-1.4	<1	<1	∼13	∼5
PS-PiQ**Pi**-1.3	<5	<5	∼25	∼25

[a]All data was obtained by integration and comparison of different signals in ¹H NMR spectra before and after immersion in 2 M NaOH (aq). The signals in the aromatic region were used as an internal reference. [b]Region I: signal from protonated tertiary amines formed by degradation reactions. [c]Region II: calculated based on the average integral of the signals from vinylic protons formed in β-Hofmann eliminations.

PiQPi-1.3 showed less than 1 and 5% ionic losses, respectively. At 120 °C, they lost ∼13 and ∼25% of the cations, respectively. The discrepancy between the level of ionic loss calculated from regions I and II for PS-PiQdm-1.4 after storage at 120 °C indicated that degradation mechanisms other than Hofmann elimination were active, *e.g.*, methyl or ring-opening substitution reactions (Scheme S1). No such discrepancy was observed for PS-PiQPi-1.3, indicating degradation only by Hofmann elimination. In comparison, the previously observed Hofmann elimination of dimethyl piperidinium cations directly attached to the backbone in poly(arylene piperidinium) AEMs reached ∼8% after 30 days under the same conditions.[12]

The spectra in Figure 4c,f exhibit one and two sets of vinylic protons for PS-PiQdm-1.4 and PS-PiQPi-1.3, respectively. Since the first set at ∼4.9 and ∼5.4 ppm was found in the spectra of both samples, these signals were assigned to vinylic protons formed in the ring-opening of the six-membered ring closest to the backbone (Scheme 2a), while the second set of
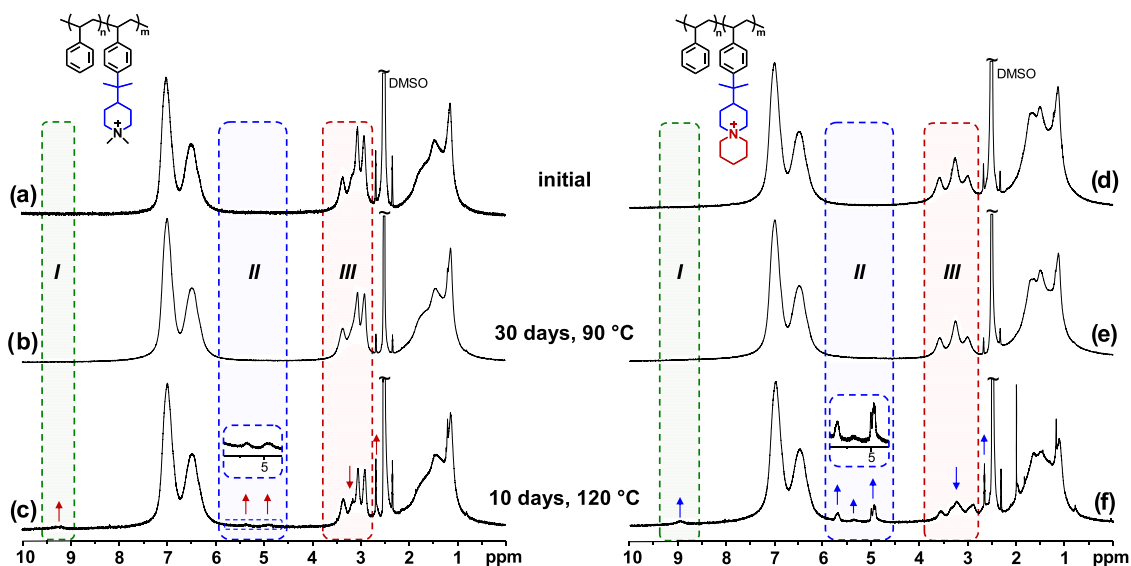
Figure 4. Selected ¹H NMR spectra of AEM samples before and after storage in 2 M aq NaOH solution at elevated temperature: (left) neat PS-PiQdm-1.4 (a), after 30 days at 90 °C (b), and after 10 days at 120 °C (c); (right) neat PS-PiQPi-1.3 (d), after 30 days at 90 °C (e), and after 10 days at 120 °C (f). Three different regions (I−III) where changes in the spectra were observed are highlighted. Changes in the spectra are marked by arrows.
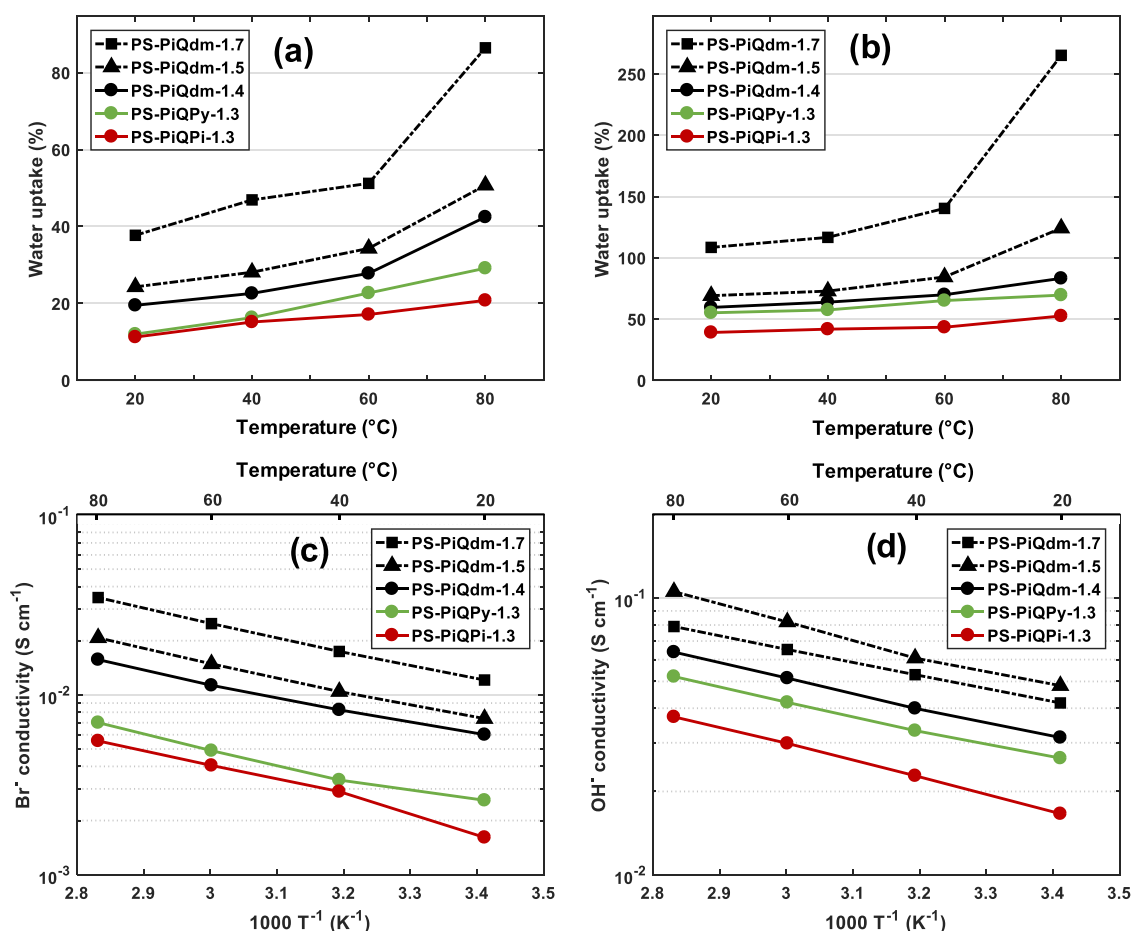
Figure 5. AEM water uptake in the Br^- (a) and OH^- (b) forms, and the corresponding Br^- (c) and OH^- (d) conductivities under fully hydrated (immersed) conditions. (Please note the different scales on the vertical axes.).

(larger) signals at ∼4.9 and ∼5.7 ppm, only found for PS-PiQPi-1.3, most likely originated from vinylic protons formed by ring-opening of the ring formed by cyclo-quaternization (in red, Scheme 2b). This observation disagreed with our previous findings on poly(arylene alkylenes) carrying *N*-spirocyclic cations, where the pendant ring was consistently observed to be more stable.[11] A reason for the higher stability of the ring attached to the backbone in the present study may be the increased hydrophobicity and steric protection introduced by the methyl groups on the benzylic carbon. The degree of Hofmann elimination observed for both mono- and *N*-spirocyclic piperidine-based cations in the current work was lower than that observed for similar cations in poly(arylene alkylene) AEMs.[11,12] This observation was most likely due to the sp^3 carbon introduced between the piperidinium ring and the polymer backbone, and the more flexible PS backbone, which allowed a more efficient ring relaxation.

The observation in region III is a general decrease in the intensity of all signals present in relation to the aromatic ones, as can be seen clearly in Figure S6, where no new emerging signals were observed. The former signals originate from protons in the α-position to the charged *N*-center and the decrease was accompanied by a decrease of signals at 1−2 ppm (Figure S6). This finding seems to be unrelated to the changes in regions I and II. As discussed above, all previously reported degradation mechanisms of the *N*-alicyclic piperidinium cation give rise to tertiary amines. Hence, the observed changes in region III were not consistent with cationic degradation.

Instead, we envisaged two possible causes, namely, the loss of a fraction of highly functionalized PS by leaching or dissolution and/or cleavage of the benzylic C−C bond and loss of the entire functional group.

As mentioned above, the Friedel−Crafts reaction proceeded in a heterogeneous system (suspension) where the PS gradually dissolved with increased functionalization. It is thus likely that the samples were inhomogeneously functionalized, resulting in a fraction with significantly higher DF than average. Hence, it is probable that fractions of the highly functionalized (and more water soluble) PS were leached out from the AEMs into the NaOH solution at the elevated temperature during the alkaline stability tests. This would result in a decrease (relative to the aromatic signals) of all of the ^1H NMR signals from the entire cationic group attached to PS in the remaining AEM sample, which explains the changes seen in region III (Figure 4) and in Figure S6. Notably, any ionic loss makes the polymers more hydrophobic and therefore decreases the solubility in aq NaOH. Consequently, it is unlikely that the polymer chains lost *via* leaching had degraded more in relation to those that remained in the AEM and were analyzed by NMR. Indeed, leaching was confirmed by studying the change in the mass of AEM samples immersed in 2 M aq NaOH at 90 °C during 30 days. After this treatment, the mass of both PS-PiQdm-1.4 and PS-PiQdm-1.7 had decreased by approximately 10 wt %. To enable analysis by NMR spectroscopy, a further experiment was performed at a reduced alkali concentration but increased temperature. Hence, PS-

PiQdm-1.4 was immersed in 0.1 M aq NaOH at 120 °C for 10 days. As expected, the ¹H NMR spectrum of the leached polymer fraction showed a substantially higher DF than the value of the original sample (Figure S7). All of the details of the leaching experiments are presented in the Supporting Information.

To exclude the possibility that a degradation mechanism exists that caused the loss of the entire functional group, a model compound [2-(dimethyl piperidinium-4-yl)propan-2-tolyl] was prepared and its molecular structure was studied after alkaline treatment during 14 days at 120 °C (Figure S8). After treatment in 2 M aq NaOH, no changes in the spectrum (Figure S8b) were observed. However, small signals indicating Hofmann elimination were identified after storage in 5 M aq NaOH (Figure S8c), but no changes indicating cleavage of the benzylic C—C bond were observed. Consequently, the study of the model compound demonstrated the high alkaline stability of the piperidinium cation and further supported that the changes observed in region III of the NMR spectra during the stability evaluation were caused by the loss of a polymer fraction with high ionic content.

As expected, the alkaline stability of both PS-PiQdm-1.4 and PS-PiQPi-1.3 was much higher than that measured for SEBS functionalized with BTMA cations, which showed significant degradation already at 60 °C.[32,33] In comparison, the alkyl-TMA functionalized SEBS reported by Bae et al. showed no signs of cation degradation after 500 h in 1 M aq NaOH at 80 °C[37] and no degradation was reported for the PS carrying N-spirocyclic cations presented by Li et al. after 3000 h at 80 °C in 1 M NaOH CD₃OD/D₂O. However, in the latter study, the presence of a large water signal, which would overlap any emerging vinyl signals present due to ring-opening Hofmann elimination, complicated the analysis.

Morphology, Water Uptake, and Ion Conductivity. The ability of the AEMs to form ionic clusters during the casting process was studied by small-angle X-ray spectroscopy (SAXS). No ionomer peak was detected in the range $q = 0.14$–8.0 nm⁻¹ for dry PS-PiQdm-1.4 and -1.7 in the Br⁻ form, as shown in Figure S4. This indicated that no ordered phase structure was formed by the ionic and nonionic units in the AEM.[45]

The water uptake of the AEMs in the Br⁻ and OH⁻ forms reached 21–86 and 53–268%, respectively, at 80 °C (Table 1 and Figure 5a,b). As expected, the water uptake increased with IEC. The PS-PiQPy-1.3 and PS-PiQPi-1.3 membranes displayed lower water uptake compared to the PS-PiQdm-1.4 membrane prepared from the same precursor polymer. This difference can be explained by the slightly lower IEC of the former AEMs and because of the more bulky character of the spiro-cations, which can be expected to prevent efficient ionic clustering and phase separation (Figure 5a,b).[14] The same trend was observed in the ion conductivity, where PS-PiQPy-1.3 and PS-PiQPi-1.3 displayed lower values in both the Br⁻ and OH⁻ forms than the corresponding dimethyl derivative (Table 1 and Figure 5c,d). PS-PiQdm-1.7 recorded the highest Br⁻ conductivity (35 mS cm⁻¹) and PS-PiQdm-1.5 reached the highest OH⁻ conductivity (106 mS cm⁻¹). This indicated that PS-PiQdm-1.7 suffered from dilution effects due to the excessive water uptake in the OH⁻ form. In general, the AEMs based on PS were mechanically weak and took up large amounts of water already at moderate IECs, despite the rather high molecular weight.

Blend Membranes. The preparation of well-tuned blend membranes is an efficient strategy to mitigate swelling issues, decrease water uptake, and improve mechanical properties.[38,46,47] By blending a cationic and an anionic polymer, strong interactions and cross-linking can be introduced through the formation of ionic complexes between the polymers.[46] These act to both reduce the effective IEC and restrict the swelling of the membrane. However, the formation of homogeneous membranes by cocasting oppositely charged polymers is difficult because the strong ionic interactions normally cause insolubility and instant precipitation. One strategy to circumvent this issue is generation of one of the charges after the casting process by protonation or deprotonation of one of the polymer components of the blend.[47]

Blend membranes of PS-PiQdm-1.7 and a commercially available polybenzimidazole (PBI-O) were prepared as a proof of concept to demonstrate AEMs based on PS functionalized with N-alicyclic piperidine-based cations with improved handling properties and reduced water uptake, as compared to the neat PS-PiQdm-y AEMs. Ionic cross-links in the form of piperidinium—imidazolate complexes (Figure 6a) were intro-
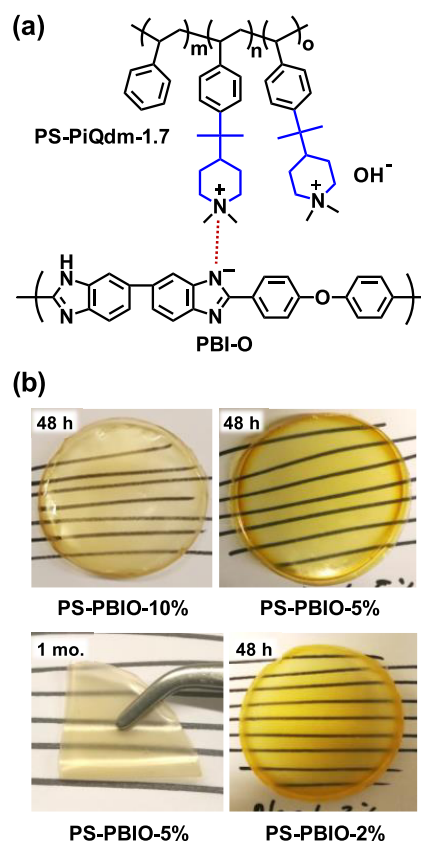
Figure 6. (a) Piperidinium—imidazolate complex forming ionic cross-links in the blend AEMs. (b) Photographs of wet blend AEMs after storage in 1 M NaOH during different periods.

duced directly after cocasting the two polymers by deprotonation of —NH— groups of the PBI-O component by immersing the blend AEMs in aq NaOH. The preparation of blend membranes through the formation of piperidinium—imidazolate complexes most probably restricts the leaching of polymer fractions with high ionic contents, as observed during the alkaline stability assessment of the neat PS-based AEMs.
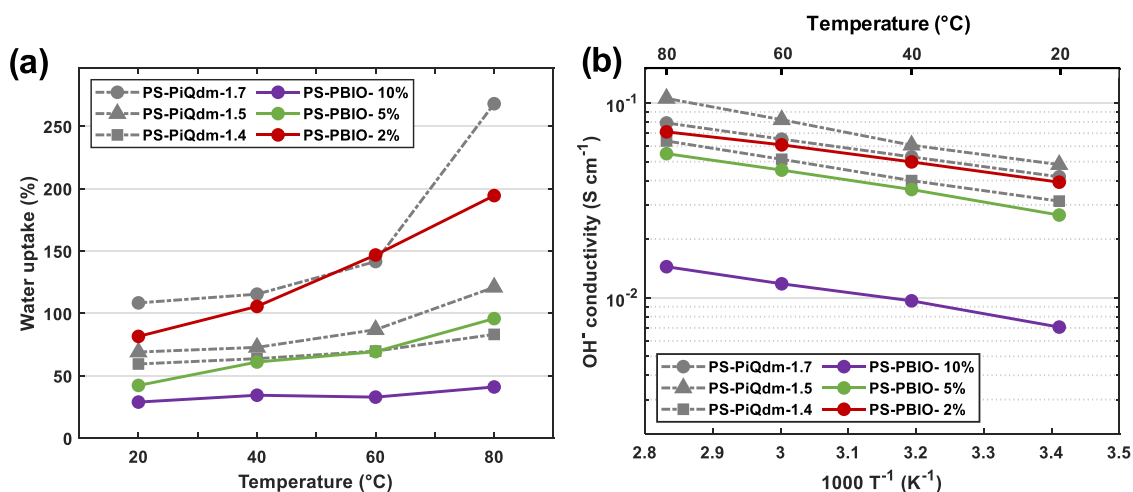
Figure 7. Water uptake (a) and conductivity (b) of the blend AEMs in the OH⁻ form measured in the fully hydrated (immersed) state. Data from the PS-PiQdm-*y* series (gray) was added for comparison.

Blend AEMs based on PS-PiQdm-1.7 containing 2, 5, and 10 wt % PBI-O (denoted PS-PBIO-2%, PS-PBIO-5%, and PS-PBIO-10%, respectively) were prepared by solvent casting from 4 wt % polymer solutions in DMSO at 80 °C. The transparent membranes were directly immersed in 1 M aq NaOH before removal from the Petri dish. To avoid dissociation of the ionic complexes, and hence dissolution of the membranes, all of the blend AEMs were stored in 1 M aq NaOH at room temperature before measurements. The strict need to keep the blend AEMs under strongly basic conditions prevented the determination of the IEC of the blend membranes using Mohr's or acid–base titration methods.

Photographs of wet blend AEMs in the OH⁻ form are shown in Figure 6b (larger size in Figure S5). Both PS-PBIO-10 and −5% were transparent after a 48 h storage in 1 M NaOH. However, PS-PBIO-2% was slightly opaque after the same treatment. PS-PBIO-5% lost some color and became more opaque during 1-month storage (compare Figure 6b, I and II) but retained its flexibility and robustness. In general, all blend AEMs showed improved handling properties in relation to PS-PiQdm-1.7. The effect of the blending on the polymer leaching was analyzed under the same conditions as those for PS-PiQdm-1.4 (0.1 M aq NaOH, 120 °C), and NMR analysis of the aq NaOH solution clearly showed the presence of a leached fraction of PS-PiQdm-1.7 (Figure S9). Hence, the ionic interactions (ionic cross-links) between the polymers in the blend did not completely prevent the leaching.

As expected, the water uptake of the blend AEMs was strongly dependent on the PBI content and increased with the theoretical IEC to reach 41, 95, and 194% for PS-PBIO-10, −5, and −2%, respectively, at 80 °C (Figure 7a). The OH⁻ conductivity of the blend AEMs, displayed in Figure 7b, also followed the IEC. At 80 °C, PS-PBIO-2% exhibited the highest water uptake (194%) and the highest OH⁻ conductivity (71 mS cm⁻¹). This may be compared with the water uptake (268%) and OH⁻ conductivity (79 mS cm⁻¹) of the neat PS-PiQdm-1.7 at 80 °C. Hence, blending with 2 and 5 wt % PBI-O decreased the water uptake by 28 and 64%, respectively, which was accompanied by 10 and 30% reductions in conductivity, respectively.

CONCLUSIONS

We have successfully attached piperidine rings to PS *via* a Friedel−Crafts alkylation reaction using commercially available Pip*t*OH in a superacidic medium. Up to approximately 30% of the styrene units were modified, and subsequent quaternizations to obtain the *N,N*-dimethyl piperidinium and spirocyclic quaternary ammonium cations were quantitative. The alkaline stability of the cations was very high and only limited degradation occurred by Hofmann elimination at 90 °C. The presence of the isopropylidene spacer in between the PS chain and the cationic rings, as well as the high chain flexibility of the backbone, mitigate Hofmann elimination in comparison with poly(arylene alkylenes) carrying similar cations. The *N,N*-dimethyl piperidinium cation was slightly more stable than the bis-6-membered quaternary ammonium cation, and the latter cation was mainly lost *via* Hofmann elimination in the ring formed by cyclo-quaternization. The AEMs showed high hydroxide conductivity despite their moderate IEC values. However, due to the general brittleness of PS derivatives, these AEMs were fragile, suffered from excessive water uptake, and a polymer fraction with high ionic content was leached out in hot alkaline solutions. Consequently, ionically cross-linked blend AEMs with PBI were prepared as a proof of concept to improve the handling properties, decrease the water uptake, and mitigate the leaching process. Here, the formation of piperidinium−imidazolate complexes facilitated the compatibility between the blend components. The blend membranes showed decreased water uptake and improved mechanical properties, accompanied by only a small reduction in conductivity. However, the leaching was not eliminated. The results of this work show that the crucial alkaline stability of PS-based AEMs can be significantly improved by replacing benchmark BTMA cations with *N*-alicyclic piperidine-based cations. This may considerably improve the feasibility of using cationic PS membranes in AEMFCs operating at elevated temperatures. Moreover, the synthetic approach presented here can be used to introduce alkali-stable piperidine-based cations into alternative polymers containing suitable phenyl groups.

EXPERIMENTAL SECTION

Materials. Polystyrene (PS, $M_n \sim$ 170 kg mol⁻¹, PDI = 2.06, Sigma-Aldrich), 2-(piperidine-4-yl)propan-2-ol (Pip*t*OH, 95%, Fluo-

rochem), 1,1,1-trifluoroacetic acid (TFA, 99%, Acros), 1,1,1-trifluoromethanesulfonic acid (TFSA, 99%, Acros), iodomethane (99%, Sigma-Aldrich), K$_2$CO$_3$ (99%, Acros), 1,5-dibromopentane (97%, Sigma-Aldrich), 1,4-dibromobutane (99%, Sigma-Aldrich), N-ethyldiisopropylamine (DIPEA, 99%, Sigma-Aldrich), isopropanol (IPA, reagent grade, VWR), diethyl ether (reagent grade, VWR), N-methyl-2-pyrrolidone (NMP, reagent grade, Acros), dimethyl sulfoxide (DMSO, reagent grade, VWR), NaBr (99%, Sigma-Aldrich), NaOH (99%, pellets, VWR), chloroform-d (99.8 atom % D, Sigma-Aldrich), and DMSO-d$_6$ (99.96 atom % D, Sigma-Aldrich) were all used as received. Dichloromethane and toluene were dried in an MBraun dry solvent dispenser system (MB-SPS 800) prior to use.

Functionalization of Polystyrene. The PS-Pix% series was prepared using a modified previously published procedure.[43] An amount of 2.58 g (18.0 mmol) of PiptOH was added in total to a solution of PS (2 g, 24.0 mmol) in dry DCM (10 mL) under nitrogen. First, 20% of the reagent was added to the polymer solution, before the solution was cooled to 0 °C in an ice bath. TFSA (3.50 mL, 39.6 mmol) was then slowly added to the reaction mixture, which turned orange and turbid. The remaining PiptOH was added portionwise using a spatula over the next 30−60 min and the reaction was continued for 1 h at 0 °C after the entire reagent had been added. The reaction mixture increased in viscosity (some reactions required additional DCM for continued stirring) and had become more homogeneous and red/maroon-colored. The reaction was terminated by pouring the reaction mixture into a 5- to 10-fold larger volume of diethyl ether under vigorous stirring. The product was washed once in ether, dried under vacuum in room temperature, and then washed several times in water before the charged precursor PS-Pix was obtained (where x is the percentage of styrene moieties carrying a piperidine calculated by ^{1}H NMR spectroscopy).

Quaternization and Cyclo-Quaternization. The precursor polymers in the PS-Pix series were completely quaternized by methylation with iodomethane, or by cyclo-quaternization using 1,5-dibromopentane or 1,4-dibromobutane. The methylation reaction to produce PS-PiQdm-1.4 was undertaken by stirring a mixture of PS-Pi19 (0.50 g, 1 equiv piperidine units), iodomethane (0.10 mL, 3 equiv), and K$_2$CO$_3$ (0.08 g, 2 equiv) in 10 mL of NMP at room temperature overnight in the dark. The yellow polymer mixture was precipitated in a tenfold solution of diethyl ether and isopropanol (90:10 v/v) and washed once in diethyl ether, quickly dried in a filter funnel, and then washed with water to remove salts and dried at 50 °C under vacuum after filtration.

PS-PiQPi-1.3 and PS-PiQPy-1.3 were prepared by cyclo-quaternization of PS-Pi19. The preparation of PS-PiQPi-1.3 is given as an example. First, PS-Pi19 (0.5 g, 1 equiv piperidine units) was dissolved in 12 mL of NMP. This solution was subsequently dropwise added into a heated solution (80 °C) of DIPEA (0.52 mL, 5 equiv) and 1,5-dibromopentane (46.4 μL, 1.1 equiv) in 4 mL of NMP. The addition occurred over 1 h, and the reaction was left stirring overnight, before precipitation and purification as described previously.

All quaternized polymers were typically obtained in 80−90% isolated yields and were off-white to yellow/orange. They were soluble in acetone, isopropanol, methanol, NMP, and DMSO but not in water, diethyl ether, or chloroform.

Preparation of Model Compound. The model compound 2-(dimethyl piperidinium-4-yl)propan-2-tolyl was prepared in two steps. First, PiptOH (0.95 g, 1 equiv) and toluene (2.0 mL, 2.5 equiv) were stirred in TFSA (5 mL, 5 equiv) at 0 °C for 2 h. Subsequently, the reaction medium was poured onto ice (~5 g), treated with ~7 equiv aq KOH, and the organic phase was extracted with ethyl acetate (3 × 5 mL), followed by washing with brine and drying with MgSO$_4$. After evaporation under vacuum, the intermediate compound, 2-(piperidine-4-yl)propan-2-tolyl, was obtained. It was used without further purification. The quaternization reaction was undertaken in water at room temperature using iodomethane (2.5 equiv) with K$_2$CO$_3$ (1.1 equiv) as the catalyst. The product formed an oil-like phase on the bottom of the reaction vessel. After 48 h, the water was decanted off and the product was dissolved in ethyl acetate, washed with brine, and dried with MgSO$_4$ before being concentrated in vacuo to form a

yellow powder of the desired product. The ^{1}H NMR spectrum is shown in Figure S7a.

Structural Characterization. The molecular structures of the different compounds and polymers were analyzed with ^{1}H NMR spectroscopy using a Bruker DR X400 spectrometer. NMR spectra were obtained at 400.13 MHz using chloroform-d (δ = 7.27 ppm) or DMSO-d$_6$ (δ = 2.50 ppm) as the solvent. In some cases, 5−10 vol % TFA was added to polymer solutions in DMSO-d$_6$ to shift the water peak. Any tertiary amines present due to incomplete quaternization or cation degradation reactions were protonated by this action and gave rise to a specific NMR shift δ = 8−10 ppm.

Membrane Preparation. The quaternized polymers in the I$^-$ or Br$^-$ form (0.10 g) were dissolved in DMSO to form 5 wt % solutions for AEM casting. All of the solutions were filtered through a Teflon syringe filter (Millex LS, 5 μm) onto glass Petri dishes (Ø = 5 cm) prior to casting at 70 °C during 48 h. The AEMs were gently peeled from the dishes after hydration and the membranes in the I$^-$ form were subsequently ion-exchanged to the Br$^-$ form by immersion in 1 M aq NaBr solution at room temperature during 5 days. Next, excess salt was removed by thorough washing with deionized water. Prior to any analysis, the AEMs were stored in deionized water during at least 48 h at room temperature. The membrane thickness was approximately 60 μm.

Preparation of Blend Membranes. PS-PiQdm-1.7 was codissolved with 2, 5, and 10 wt % of PBI-O in DMSO (4 wt % solutions). Blend membranes were then cast at 80 °C during 72 h. The resulting membranes were directly treated with 1 M NaOH to deprotonate a fraction of the imidazole units in the PBI-O and were then stored under the same conditions at room temperature for 48 h before any measurements. The alkaline solution was replaced twice during this time. Prior to water uptake and conductivity measurements, the membranes were treated as described previously. As the excess NaOH aq was washed away, ionic cross-links (piperidinium−imidazolate complexes) were formed, improving the mechanical properties of the membranes as well as decreasing the IEC. The IEC of the membranes could not be characterized using titrations since that would require neutral or acidic pH, which would compromise the blend AEMs.

Thermal Characterization. A TA Instruments TGA Q500 was utilized to study thermal decomposition. Traces of water in the samples were removed by preheating at 110 °C during 10 min before analysis. All measurements were performed at a heating rate of 10 °C min^{-1} from 50 to 600 °C under N$_2$. The thermal decomposition temperature ($T_{d,95}$) was determined at 5% weight loss. To study glass transitions (T_gs), differential scanning calorimetry (DSC, TA Instruments Q2000) was utilized. The samples were analyzed in two heating steps: from 20 to 175 and 50 to 200 °C. The T_g was taken from the inflexion point in the thermogram during the second heating step.

Ion-Exchange Capacity (IEC) and Water Uptake. Mohr titrations were used to determine the IEC of the AEMs in the Br$^-$ form. First, samples were dried under vacuum at 50 °C for at least 40 h and weighed before storage and ion-exchange in 0.2 M aq NaNO$_3$ (25.00 mL) during 48 h at ~50 °C. Four 5.00 mL samples of the resulting solutions were titrated with 0.01 M aq AgNO$_3$ using K$_2$CrO$_4$ as the colorimetric indicator and the IEC was calculated from the average endpoint.

The water uptake of the AEMs was characterized gravimetrically. To obtain the dry weight of the AEMs in the Br$^-$ form (W_{Br^-}), the samples were dried as described above. The samples were ion-exchanged to the OH$^-$ form by immersion in ~1 M NaOH during 48 h at ambient temperature. Subsequently, the membranes were repeatedly washed with degassed and deionized water in a desiccator (CO$_2$-free environment) during at least 48 h. The pH of the washing water was monitored. The samples were equilibrated for 6 h at 40, 60, and 80 °C, respectively; then, the samples were wiped with tissue paper to remove excess water and the weight of the swollen sample (W'_{OH^-}) was obtained. The dry weight of the membrane in the OH$^-$ form (W_{OH^-}) was calculated using the titrated IEC values and W_{Br^-} and the water uptake (WU) was then calculated as

$$WU = \frac{W'_{OH^-} - W_{OH^-}}{W_{OH^-}}$$

Conductivity Measurements. The ion conductivity of all of the AEMs was determined in the fully hydrated state in a sealed cell by electrochemical impedance spectroscopy. The measurements were carried out between 20 and 80 °C, in steps of 20 °C, in a Novocontrol high-resolution dielectric analyzer V 1.01S at 50 mV and 10^0–10^7 Hz. AEM pieces in the Br^- form were ion-exchanged to the OH^- form and then washed thoroughly to remove any residual OH^- ions as described above. To avoid carbonate formation, this process was undertaken in an environment free of CO_2, e.g., in degassed deionized water under nitrogen protection.

Small-Angle X-ray Scattering (SAXS). The morphology of dry AEMs in the Br^- form was studied in a SAXSLAB ApS system (JJ X-ray, Denmark) combined with a Pilatus detector. The measurements were undertaken at a q-range of 0.14–8.0 nm^{-1}, using Cu radiation ($K\alpha$, 1.542 Å).

Evaluation of AEM Stability in an Alkaline Solution. To quantify ionic loss and assess the active degradation mechanisms, the molecular structures of AEM samples were studied by ^{1}H NMR spectroscopy before and after storage in alkaline media. Samples were immersed in 2 M aq NaOH at 90 and 120 °C, respectively, and kept in sealed containers with Teflon inserts. At regular periods of time, sample pieces were taken out and ion-exchanged to the Br^- form, washed, dried, and analyzed by ^{1}H NMR spectroscopy as described above.

■ ASSOCIATED CONTENT

ⓢ Supporting Information

The Supporting Information is available free of charge at https://pubs.acs.org/doi/10.1021/acs.macromol.0c00201.

> Polymer NMR spectra, DSC, TGA, and SAXS data; photographs of blend membranes; and a scheme of typical degradation mechanisms for *N*-alicyclic QA cations (PDF)

■ AUTHOR INFORMATION

Corresponding Author

    Patric Jannasch − *Polymer & Materials Chemistry, Department of Chemistry, Lund University, SE-221 00 Lund, Sweden;* ⓞ orcid.org/0000-0002-9649-7781; Email: patric.jannasch@chem.lu.se

Authors

    Joel S. Olsson − *Polymer & Materials Chemistry, Department of Chemistry, Lund University, SE-221 00 Lund, Sweden;* ⓞ orcid.org/0000-0002-4193-6986

    Thanh Huong Pham − *Polymer & Materials Chemistry, Department of Chemistry, Lund University, SE-221 00 Lund, Sweden;* ⓞ orcid.org/0000-0002-2063-8461

Complete contact information is available at:
https://pubs.acs.org/10.1021/acs.macromol.0c00201

Notes

The authors declare no competing financial interest.

■ ACKNOWLEDGMENTS

■ REFERENCES

(1) Varcoe, J. R.; Atanassov, P.; Dekel, D. R.; Herring, A. M.; Hickner, M. A.; Kohl, P. A.; Kucernak, A. R.; Mustain, W. E.; Nijmeijer, K.; Scott, K.; Xu, T.; Zhuang, L. Anion-Exchange Membranes in Electrochemical Energy Systems. *Energy Environ. Sci.* **2014**, *7*, 3135.

(2) Varcoe, J. R.; Slade, R. C. T. Prospects for Alkaline Anion-Exchange Membranes in Low Temperature Fuel Cells. *Fuel Cells* **2005**, *5*, 187−200.

(3) Gottesfeld, S.; Dekel, D. R.; Page, M.; Bae, C.; Yan, Y.; Zelenay, P.; Kim, Y. S. Anion exchange membrane fuel cells: Current status and remaining challenges. *J. Power Sources* **2018**, *375*, 170−184.

(4) Dekel, D. R. Review of cell performance in anion exchange membrane fuel cells. *J. Power Sources* **2018**, *375*, 158−169.

(5) Arges, C. G.; Zhang, L. Anion Exchange Membranes' Evolution toward High Hydroxide Ion Conductivity and Alkaline Resiliency. *ACS Appl. Energy Mater.* **2018**, *1*, 2991−3012.

(6) You, W.; Noonan, K. J. T.; Coates, G. W. Alkaline-stable anion exchange membranes: A review of synthetic approaches. *Prog. Polym. Sci.* **2020**, *100*, No. 101177.

(7) Choi, C.; Kim, S.; Kim, R.; Choi, Y.; Kim, S.; Jung, H.-Y.; Yang, J. H.; Kim, H.-T. A review of vanadium electrolytes for vanadium redox flow batteries. *Renewable Sustainable Energy Rev.* **2017**, *69*, 263−274.

(8) Marino, M. G.; Kreuer, K. D. Alkaline Stability of Quaternary Ammonium Cations for Alkaline Fuel Cell Membranes and Ionic Liquids. *ChemSusChem* **2015**, *8*, 513−523.

(9) Mohanty, A. D.; Bae, C. Mechanistic analysis of ammonium cation stability for alkaline exchange membrane fuel cells. *J. Mater. Chem. A* **2014**, *2*, 17314−17320.

(10) Hugar, K. M.; Kostalik, H. A.; Coates, G. W. Imidazolium Cations with Exceptional Alkaline Stability: A Systematic Study of Structure−Stability Relationships. *J. Am. Chem. Soc.* **2015**, *137*, 8730.

(11) Pham, T. H.; Olsson, J. S.; Jannasch, P. Poly(arylene alkylene)s with pendant N-spirocyclic quaternary ammonium cations for anion exchange membranes. *J. Mater. Chem. A* **2018**, *6*, 16537−16547.

(12) Olsson, J. S.; Pham, T. H.; Jannasch, P. Poly(arylene piperidinium) Hydroxide Ion Exchange Membranes: Synthesis, Alkaline Stability, and Conductivity. *Adv. Funct. Mater.* **2017**, *28*, No. 1702758.

(13) Allushi, A.; Pham, T. H.; Olsson, J. S.; Jannasch, P. Ether-free polyfluorenes tethered with quinuclidinium cations as hydroxide exchange membranes. *J. Mater. Chem. A* **2019**, *7*, 27164−27174.

(14) Pham, T. H.; Olsson, J. S.; Jannasch, P. Effects of the N-alicyclic cation and backbone structures on the performance of poly(terphenyl)-based hydroxide exchange membranes. *J. Mater. Chem. A* **2019**, *7*, 15895−15906.

(15) Mohanty, A. D.; Tignor, S. E.; Krause, J. A.; Choe, Y.-K.; Bae, C. Systematic Alkaline Stability Study of Polymer Backbones for Anion Exchange Membrane Applications. *Macromolecules* **2016**, *49*, 3361−3372.

(16) Lee, W.-H.; Park, E. J.; Han, J.; Shin, D. W.; Kim, Y. S.; Bae, C. Poly(terphenylene) Anion Exchange Membranes: The Effect of Backbone Structure on Morphology and Membrane Property. *ACS Macro Lett.* **2017**, *6*, 566−570.

(17) Lee, W.-H.; Kim, Y. S.; Bae, C. Robust Hydroxide Ion Conducting Poly(biphenyl alkylene)s for Alkaline Fuel Cell Membranes. *ACS Macro Lett.* **2015**, *4*, 814−818.

(18) Yan, Y.; Xu, B.; Wang, J.; Zhao, Y. Poly(aryl piperidinium) Polymers for Use as Hydroxide Exchange Membranes and Ionomers. U.S. Patent US10,290,8902019.

(19) Peng, H.; Li, Q.; Hu, M.; Xiao, L.; Lu, J.; Zhuang, L. Alkaline polymer electrolyte fuel cells stably working at 80 °C. *J. Power Sources* **2018**, *390*, 165−167.

(20) Olsson, J. S.; Pham, T. H.; Jannasch, P. Tuning poly(arylene piperidinium) anion-exchange membranes by copolymerization, partial quaternization and crosslinking. *J. Membr. Sci.* **2019**, *578*, 183−195.

(21) Chen, W.; Mandal, M.; Huang, G.; Wu, X.; He, G.; Kohl, P. A. Highly Conducting Anion-Exchange Membranes Based on Cross-Linked Poly(norbornene): Ring Opening Metathesis Polymerization. *ACS Appl. Energy Mater.* **2019**, *2*, 2458−2468.

(22) Mandal, M.; Huang, G.; Kohl, P. A. Highly Conductive Anion-Exchange Membranes Based on Cross-Linked Poly(norbornene): Vinyl Addition Polymerization. *ACS Appl. Energy Mater.* **2019**, *2*, 2447−2457.

(23) Huang, G.; Mandal, M.; Peng, X.; Yang-Neyerlin, A. C.; Pivovar, B. S.; Mustain, W. E.; Kohl, P. A. Composite Poly-(norbornene) Anion Conducting Membranes for Achieving Durability, Water Management and High Power (3.4 W/cm2) in Hydrogen/Oxygen Alkaline Fuel Cells. *J. Electrochem. Soc.* **2019**, *166*, F637−F644.

(24) Wang, C.; Mo, B.; He, Z.; Shao, Q.; Pan, D.; Wujick, E.; Guo, J.; Xie, X.; Xie, X.; Guo, Z. Crosslinked norbornene copolymer anion exchange membrane for fuel cells. *J. Membr. Sci.* **2018**, *556*, 118−125.

(25) Ponce-González, J.; Whelligan, D. K.; Wang, L.; Bance-Soualhi, R.; Wang, Y.; Peng, Y.; Peng, H.; Apperley, D. C.; Sarode, H. N.; Pandey, T. P.; Divekar, A. G.; Seifert, S.; Herring, A. M.; Zhuang, L.; Varcoe, J. R. High performance aliphatic-heterocyclic benzyl-quaternary ammonium radiation-grafted anion-exchange membranes. *Energy Environ. Sci.* **2016**, *9*, 3724−3735.

(26) Varcoe, J. R.; Slade, R. C. T.; Lam How Yee, E.; Poynton, S. D.; Driscoll, D. J.; Apperley, D. C. Poly(ethylene-co-tetrafluoroethylene)-Derived Radiation-Grafted Anion-Exchange Membrane with Properties Specifically Tailored for Application in Metal-Cation-Free Alkaline Polymer Electrolyte Fuel Cells. *Chem. Mater.* **2007**, *19*, 2686−2693.

(27) Wang, L.; Brink, J. J.; Varcoe, J. R. The first anion-exchange membrane fuel cell to exceed 1 W cm−2 at 70 °C with a non-Pt-group (O2) cathode. *Chem. Commun.* **2017**, *53*, 11771−11773.

(28) Wang, L.; Bellini, M.; Miller, H. A.; Varcoe, J. R. A high conductivity ultrathin anion-exchange membrane with 500+ h alkali stability for use in alkaline membrane fuel cells that can achieve 2 W cm−2 at 80 °C. *J. Mater. Chem. A* **2018**, *6*, 15404−15412.

(29) Sun, L.; Guo, J.; Zhou, J.; Xu, Q.; Chu, D.; Chen, R. Novel nanostructured high-performance anion exchange ionomers for anion exchange membrane fuel cells. *J. Power Sources* **2012**, *202*, 70−77.

(30) Dai, P.; Mo, Z.-H.; Xu, R.-W.; Zhang, S.; Wu, Y.-X. Cross-Linked Quaternized Poly(styrene-b-(ethylene-co-butylene)-b-styrene) for Anion Exchange Membrane: Synthesis, Characterization and Properties. *ACS Appl. Mater. Interfaces* **2016**, *8*, 20329−20341.

(31) Hao, J.; Gao, X.; Jiang, Y.; Zhang, H.; Luo, J.; Shao, Z.; Yi, B. Crosslinked high-performance anion exchange membranes based on poly(styrene-b-(ethylene-co-butylene)-b-styrene). *J. Membr. Sci.* **2018**, *551*, 66−75.

(32) Wang, Z.; Parrondo, J.; Ramani, V. Anion Exchange Membranes Based on Polystyrene-Block-Poly(ethylene-ran-buty-lene)-Block-Polystyrene Triblock Copolymers: Cation Stability and Fuel Cell Performance. *J. Electrochem. Soc.* **2017**, *164*, F1216−F1225.

(33) Gao, X.; Yu, H.; Qin, B.; Jia, J.; Hao, J.; Xie, F.; Shao, Z. Enhanced water transport in AEMs based on poly(styrene−ethylene−butylene−styrene) triblock copolymer for high fuel cell performance. *Polym. Chem.* **2019**, *10*, 1894−1903.

(34) Nuñez, S. A.; Capparelli, C.; Hickner, M. A. N-Alkyl Interstitial Spacers and Terminal Pendants Influence the Alkaline Stability of Tetraalkylammonium Cations for Anion Exchange Membrane Fuel Cells. *Chem. Mater.* **2016**, *28*, 2589−2598.

(35) Tomoi, M.; Yamaguchi, K.; Ando, R.; Kantake, Y.; Aosaki, Y.; Kubota, H. Synthesis and thermal stability of novel anion exchange resins with spacer chains. *J. Appl. Polym. Sci.* **1997**, *64*, 1161−1167.

(36) Jeon, J. Y.; Mohanty, A. D.; Tian, D.; Bae, C. Ionic Functionalization of Polystyrene-b-poly(ethylene-co-butylene)-b-polystyrene via Friedel-Crafts Bromoalkylation and Its Application for Anion Exchange Membranes. *ECS Trans.* **2017**, 967−970.

(37) Jeon, J. Y.; Park, S.; Han, J.; Maurya, S.; Mohanty, A. D.; Tian, D.; Saikia, N.; Hickner, M. A.; Ryu, C. Y.; Tuckerman, M. E.; Paddison, S. J.; Kim, Y. S.; Bae, C. Synthesis of Aromatic Anion Exchange Membranes by Friedel−Crafts Bromoalkylation and Cross-Linking of Polystyrene Block Copolymers. *Macromolecules* **2019**, *52*, 2139−2147.

(38) Wang, X.; Sheng, W.; Shen, Y.; Liu, L.; Dai, S.; Li, N. N-cyclic quaternary ammonium-functionalized anion exchange membrane with improved alkaline stability enabled by aryl-ether free polymer backbones for alkaline fuel cells. *J. Membr. Sci.* **2019**, *587*, No. 117135.

(39) Dang, H.-S.; Jannasch, P. Exploring Different Cationic Alkyl Side Chain Designs for Enhanced Alkaline Stability and Hydroxide Ion Conductivity of Anion-Exchange Membranes. *Macromolecules* **2015**, *48*, 5742−5751.

(40) Dang, H.-S.; Weiber, E. A.; Jannasch, P. Poly(phenylene oxide) functionalized with quaternary ammonium groups via flexible alkyl spacers for high-performance anion exchange membranes. *J. Mater. Chem. A* **2015**, *3*, 5280−5284.

(41) Park, E. J.; Maurya, S.; Hibbs, M. R.; Fujimoto, C. H.; Kreuer, K.-D.; Kim, Y. S. Alkaline Stability of Quaternized Diels−Alder Polyphenylenes. *Macromolecules* **2019**, *52*, 5419−5428.

(42) Akiyama, R.; Yokota, N.; Otsuji, K.; Miyatake, K. Structurally Well-Defined Anion Conductive Aromatic Copolymers: Effect of the Side-Chain Length. *Macromolecules* **2018**, *51*, 3394−3404.

(43) Jeon, J. Y.; Umstead, Z.; Kangovi, G. N.; Lee, S.; Bae, C. Functionalization of Syndiotactic Polystyrene via Superacid-Catalyzed Friedel−Crafts Alkylation. *Top. Catal.* **2018**, *61*, 610−615.

(44) Olsson, J. S.; Pham, T. H.; Jannasch, P. Poly(N,N-diallylazacycloalkane)s for Anion-Exchange Membranes Functionalized with N-Spirocyclic Quaternary Ammonium Cations. *Macromolecules* **2017**, *50*, 2784−2793.

(45) Gebel, G.; Diat, O. Neutron and X-ray Scattering: Suitable Tools for Studying Ionomer Membranes. *Fuel Cells* **2005**, *5*, 261−276.

(46) Thomas, O. D.; Soo, K. J. W. Y.; Peckham, T. J.; Kulkarni, M. P.; Holdcroft, S. A Stable Hydroxide-Conducting Polymer. *J. Am. Chem. Soc.* **2012**, *134*, 10753−10756.

(47) Pham, T. H.; Olsson, J. S.; Jannasch, P. N-Spirocyclic Quaternary Ammonium Ionenes for Anion-Exchange Membranes. *J. Am. Chem. Soc.* **2017**, *139*, 2888−2891.